ATMOSPHERIC EFFECTS ON THE RISETIME AND WAVESHAPE OF SONIC BOOMS

Richard Raspet, Henry E. Bass and Patrice Boulanger
Department of Physics and Astronomy
University of Mississippi
University, MS 38677

ABSTRACT

Accurate prediction of human response to sonic booms from proposed HSCT aircraft depends on a knowledge of the waveshape and risetime of the boom at the ground. In previous work, we have developed a numerical technique to predict the combined effects of molecular absorption and finite wave distortion on the sonic boom as it propagates from the aircraft to the top of the turbulent boundary layer. We have more recently developed a scattering center based model to calculate the effects of turbulence on the sonic boom waveform as it propagates through this boundary layer. Calculations have been performed using single scales of turbulence and compared to measurements at Edwards AFB in the late 1960s. A model of the atmosphere involving two scales each for convective and mechanical turbulence has been developed and fit to meteorological data collected during JAPE 2. Scattering calculations employing this model underpredict the number of unperturbed waveforms. In order to develop a more realistic model of the atmosphere, the JAPE 2 meteorological data has been fit to a von Karman spectrum. Results of scattering using this multi-scale model will be presented. The combination of finite wave effects with turbulent scattering predictions includes the principal effects of the atmosphere on the sonic boom from the HSCT.

INTRODUCTION

The prediction of the average environmental impact of the HSCT requires accurate modeling of the processes affecting the sonic boom waveform and risetime. We have used the enhanced Anderson algorithm to predict the risetime and waveshape of sonic booms under non-turbulent conditions. This method can also be used to predict the risetime and waveshape at the top of the turbulent planetary boundary layer.

The enhanced Anderson algorithm includes all finite wave effects and the vibrational relaxation effects of N_2, O_2, and CO_2 in combination with atmospheric H_2O. This algorithm has been compared to data from explosions[1] and sonic booms[2] and has been tested against measurements of high intensity ballistic waves from rifles and from tank guns[3]. In addition, the results of this calculation for quasi steady shocks agree with the results from the enhanced Burgers' Equation[4,5].

Figure 1 presents the results of the application of the enhanced Anderson algorithm to a predicted HSCT waveform[6]. We emphasize that the key parameter in determining the risetime of the sonic boom is the absolute humidity.

Under turbulent conditions, the risetimes of sonic booms are scattered and are occasionally as large as ten times the risetimes calculated from vibrational relaxation considerations. It is clear that turbulence is the cause of the increased risetime and peculiar waveforms observed. Analytic techniques have been used to estimate the increase in average risetimes[7, 8, 9] and to calculate perturbed waveforms due to focusing and defocusing of the waves by turbulence[10]. In such calculations, it is usually necessary to assume a single strength and turbulence scale representative of the atmospheric turbulence. The largest turbulence effects are usually identified when the largest scales are chosen as typical.

We have chosen a different approach to calculating the effects of turbulence on sonic boom risetimes and waveforms based on a simple scattering center-based theory. The scattering center-based method accurately predicted the effects of turbulence on the coherence of continuous wave signals above natural ground surfaces[11].

METHOD

The scattering center-based technique resolves atmospheric fluctuations into a sum of discrete spherically symmetric Gaussian "turbules". The total effect of the atmosphere is then calculated by summing up the scattering amplitudes. See Figure 2. The scattered amplitudes are calculated using the first Born approximation. If the complex pressure at the receiver is written as:

$$\vec{p}^{B}(\vec{r}) = \vec{p}_o(\vec{r}) + \sum_{i=1}^{N} \vec{\psi}_i^{B} \tag{1}$$

where the superscript B refers to the first Born approximation, $\vec{p}_o(\vec{r})$ is the unperturbed spherical wave, and N is the number of turbules, then

$$\vec{\psi}_i^{B} = \frac{\sqrt{\pi}}{2} q_i k^2 s^3 \frac{e^{ik(r_{st}+r_{tr})}}{r_{st}+r_{tr}} \left[\frac{1}{1 - ia}\right] e^{-Ck^2s^2/4} \tag{2}$$

where

$$C = (1 - \cos\theta_o)^2 + \sin^2\theta_o \left[\frac{1}{1 - ia}\right] \tag{3}$$

and

$$a = \frac{ks^2}{2}\left[\frac{1}{r_{st}} + \frac{1}{r_{tr}}\right] . \tag{4}$$

s defines the $1/e^2$ contour of the turbule, q_i is the index of refraction profile strength, and θ_o is the scattering angle. The geometry is indicated in Figure 3.

The initial research on continuous wave propagation modeled the atmosphere as a random sum of identical turbules. This single scale calculation was extended to impulse propagation with promising results.[12] The impulse is Fourier transformed into the frequency domain and the total scattered component at each frequency is calculated. Then the inverse Fourier transform yields the time domain waveform. The single scale calculation (s = 10m, 30m or 100m) with a fluctuating index of refraction of $\langle\mu^2\rangle = 10 \times 10^{-6}$ predicted spiked and rounded waveforms and predicted risetimes as large as 10 ms. These results encouraged us to analyze the results of the JAPE-2 tests[13,14] using the scattering center-based model.

ANALYSIS OF JAPE-2 DATA

The JAPE-2 tests consisted of simultaneous measurement of sonic boom characteristics and meteorological measurements. The wind and temperature fluctuations were measured at heights up to 30m using sonic anemometers and hot wire anemometers. The sonic boom data was analyzed by Willshire, Garber and DeVilbiss[14] and provided as computer files. The turbulence data was analyzed by Bass, Boulanger, Olsen and Chintawongvanich[15].

a.) Two Scale Model

Examination of the data showed that a single scale model of the atmosphere could not fully describe the turbulence above the ground. The time correlation of the fluctuation quantities was fit to a two scale model. See Figure 4. Table I displays the results of the analysis for a moderately turbulent day during JAPE-2.

Table I. Example of the Two Scale Model Applied to Atmospheric Data

	Wind driven 1	Wind driven 2	Temp. driven 1	Temp. driven 2
Size (meters)	117	11	74	8
Number of Eddies	1	90	1	233
$\langle \mu^2 \rangle$	$0.54\ 10^{-5}$	$0.25\ 10^{-5}$	$0.5\ 10^{-6}$	$0.4\ 10^{-6}$

The scattering calculation was performed by summing the results of four calculations - one for each scale size. The input waveform to the scattering calculation was an N-wave propagated from the flight altitude to the top of the turbulent layer using the enhanced Anderson algorithm. The results of the Anderson algorithm agree moderately with the measurements taken under low turbulence conditions. See Table II.

Table II. Comparison of Measured and Predicted Waveform Parameters for the T-38

	Measurements for the low turbulence case	Calculations using the Anderson algorithm
Peak overpressure (psf)	0.71	0.88
Risetime (ms)	0.32	0.33

Figure 5 compares the results of the measurement and prediction for T-38 overflights under moderate turbulence conditions. Although the scattering center model produces a wide distribution of risetimes, it does not predict the shift of the histogram maximum to 2 ms; rather the maximum remains at the unperturbed value of 0.3 ms. It is believed that this is due to the use of two relatively large scales to represent the atmospheric turbulence. The scattering from large turbules is predominantly in the forward direction, and large turbules are relatively sparse, so that it is easy to "miss" the receiver with

the scattered wave. The four scale model does, however, represent a significant improvement over the single scale model.

b.) von Karman Spectrum Model

The fit of the autocorrelation to two scales rather than one improved the prediction of risetimes significantly. The high occurrence of unperturbed risetimes indicated that smaller and intermediate scales were needed to fully describe the scattering of sonic booms by turbulence.

De Wolf[16] presented a technique for simulation of a turbulent atmosphere obeying the von Karman spectrum in terms of the number density of turbules.

The general form of a 3-D von Karman spectrum is given in terms of frequency by:

$$\phi(f) = \frac{a f^2}{\left(f^2 + b\right)^{\frac{11}{6}}} \tag{5}$$

where:

$$a = 4\pi\gamma C_\varepsilon^2 \left(\frac{c}{2\pi}\right)^{2/3} \tag{6}$$

and

$$b = \left(\frac{c}{2\pi L_o}\right)^2 \tag{7}$$

The coefficients a and b are determined by fitting a function $\phi(f)$ through the measured spectra. See Figure 6.

The fit parameters are then used to determine n (s), the number density of turbules of size s needed to model the fluctuating atmosphere. De Wolf's model was originally developed to predict second moments of a scattered field and therefore is designed to reproduce only second moments of the fluctuation fields. Higher moments must be accurately represented to express the temporal characteristics of an impulse. De Wolf used an index of refraction maximum for each turbule of $\pm$ 1.0 and employed a very sparse distribution. We have varied the product of q_i^2 and n (s) until the model distribution approximates the measured second and fourth moments $\langle\mu^2\rangle = 9.6 \times 10^{-6}$, $\langle\mu^4\rangle = 2.5 \times 10^{-10}$. The variation of calculated $\langle\mu^2\rangle$ with number of turbules and q_i^2 is shown in Table III.

Table III. Calculate $<\mu^2>$ and $<\mu^4>$ as a Function of Number of Turbules

Number of Turbules	Percentage of Volume	q_i^2	$\langle\mu^2\rangle$	$\langle\mu^4\rangle$
42000	8	$1.5\ 10^{-4}$	$1.2\ 10^{-5}$	$1.0\ 10^{-9}$
63000	12	$1.0\ 10^{-4}$	$1.1\ 10^{-5}$	$1.0\ 10^{-9}$
95000	18	$6.7\ 10^{-5}$	$1.0\ 10^{-5}$	$6.9\ 10^{-10}$
127000	24	$5.0\ 10^{-5}$	$1.1\ 10^{-5}$	$5.5\ 10^{-10}$
254000	48	$2.5\ 10^{-5}$	$9.9\ 10^{-6}$	$4.4\ 10^{-10}$

The turbule spatial and size distribution for each realization is determined by Monte Carlo methods. The index of refraction fluctuations along a straight line has been compared to the corresponding measured values and exhibits similar fluctuation scales and displacement.

The second improvement to the scheme was the use of the measured height of the Planetary Boundary Layer in the calculation. Figure 7 displays the temperature versus height curve for one flight during JAPE-2. One sounding is taken with the tethesonde going up and the inversion height is 400m, the other trace is the tethesonde coming down 30 minutes later and the inversion height is at 670m. The turbulent layer thickness at the time of the later sonic boom measurement was extrapolated from this as 750m.

The results of this calculation for 20 realizations are displayed in Figure 8. The maximum occurrence risetime shows a shift away from the non-turbulent risetime of 0.3 ms. The smaller and intermediate scales of turbulence have a significant effect on the risetimes of sonic booms. It is clear, however, that the shift is not large enough to match the measured data in Figure 5a.

CONCLUSION

The enhanced Anderson algorithm provides a good prediction of waveshape and risetime of the HSCT at the top of the Planetary Boundary Layer.

The scattering center-based model can be extended to predict distorted wave shapes and longer risetimes. At this stage, the scattering based model does not predict long enough average risetimes, but does show that smaller and intermediate scales are important in increasing the average risetimes.

The larger scales are the source of the dramatically distorted waveforms, but are not the source of the shift in average risetimes. The scattering center-based calculation allows the quantitative investigation and modeling of the turbulence effects discussed qualitatively by Crow, Plotkin and George, and Pierce.

REFERENCES

1. Bass, H. E.; and Raspet, Richard: Vibrational relaxation effects on the atmospheric attenuation and risetimes of explosion waves. *J. Acoust. Soc. Am.*, vol. 64, 1978, pp. 1208-1210.

2. Bass, H. E.; Ezell, J.; and Raspet, R.: Effect of vibrational relaxation on risetime of shock waves in the atmosphere. *J. Acoust. Soc. Am.*, vol. 74, 1983, pp. 1514-1517.

3. Bass, H. E.; Layton, B. A.; Bolen, L. N.; and Raspet, R.: Propagation of medium strength shock waves through the atmosphere. *J. Acoust. Soc. Am.*, vol. 82, 1987, pp. 306-310.

4. Bass, Henry E.; and Raspet, Richard: Comparison of sonic boom risetime prediction techniques. *J. Acoust. Soc. Am.*, vol. 91, 1992, pp. 1761-1768.

5. Kang, J.; and Pierce, A. D.: Contribution of molecular relaxation to rise time of sonic booms. *J. Acoust. Soc. Am.*, Supp. 1, vol. 85, 1989, p. S81.

6. Raspet, Richard; and Bass, Henry E.: Comparison of Shock Rise Time Prediction Techniques. AIAA 13th Aeroacoustics Conference, Tallahassee, FL, Oct. 22-24, 1990.

7. Crow, S. C.: Distortion of sonic bangs by atmospheric turbulence. *J. Fluid Mech.*, vol. 37, 1969, pp. 529-563.

8. Plotkin, Kenneth J.; and George, A. R.: Propagation of weak shock waves through turbulence. *J. Fluid Mech.*, vol. 54, 1972, pp. 449-467.

9. Pierce, A. D.: Statistical theory of atmospheric turbulence effects on sonic boom rise times. *J. Acoust. Soc. Am.*, vol. 49, 1971, pp. 906-924.

10. Pierce, Allan D.: Spikes on sonic boom pressure waveforms. *J. Acoust. Soc. Am.*, vol. 44, 1968, pp. 1052-1061.

11. McBride, Walton E.; Bass, Henry E.; Raspet, Richard; and Gilbert, Kenneth E.: Scattering of sound by atmospheric turbulence: A numerical simulation above a complex impedance boundary. *J. Acoust. Soc. Am.*, vol. 90, 1991, pp. 3314-3325.

12. Raspet, Richard; Bass, Henry E.; Yao, Lixin; Boulanger, Patrice; and McBride, Walton E.: Statistical and numerical study of the relationship between turbulence and sonic boom characteristics. *J. Acoust. Soc. Am.*, Revised manuscript submitted, March, 1994.

13. Kennedy, Bruce W.; Willshire, Jr., William L.; and Olsen, Robert O.: Sonic Boom Propagation Test. The Bionetics Corporation, Las Cruces, NM, Sept., 1991.

14. Willshire, Jr., William L.; Garber, Donald P.; and DeVilbiss, David W.: Flight test measurements of the effect of turbulence on sonic boom peak overpressure and rise time. *J. Acoust. Soc. Am.*, vol. 92, 1992, p. 2329.

15. Bass, Henry E.; Boulanger, Patrice; Olsen, Robert; and Chintawongvanich, Prasan: Sonic Boom Propagation Test - Low Level Turbulence Report. Physical Acoustics Research Group Report, University of Mississippi, Feb., 1993.

16. De Wolf, D. A.: A random-motion model of fluctuation in a nearly transparent medium. *Radio Science*, vol. 18 (2), 1983, pp. 138-142.

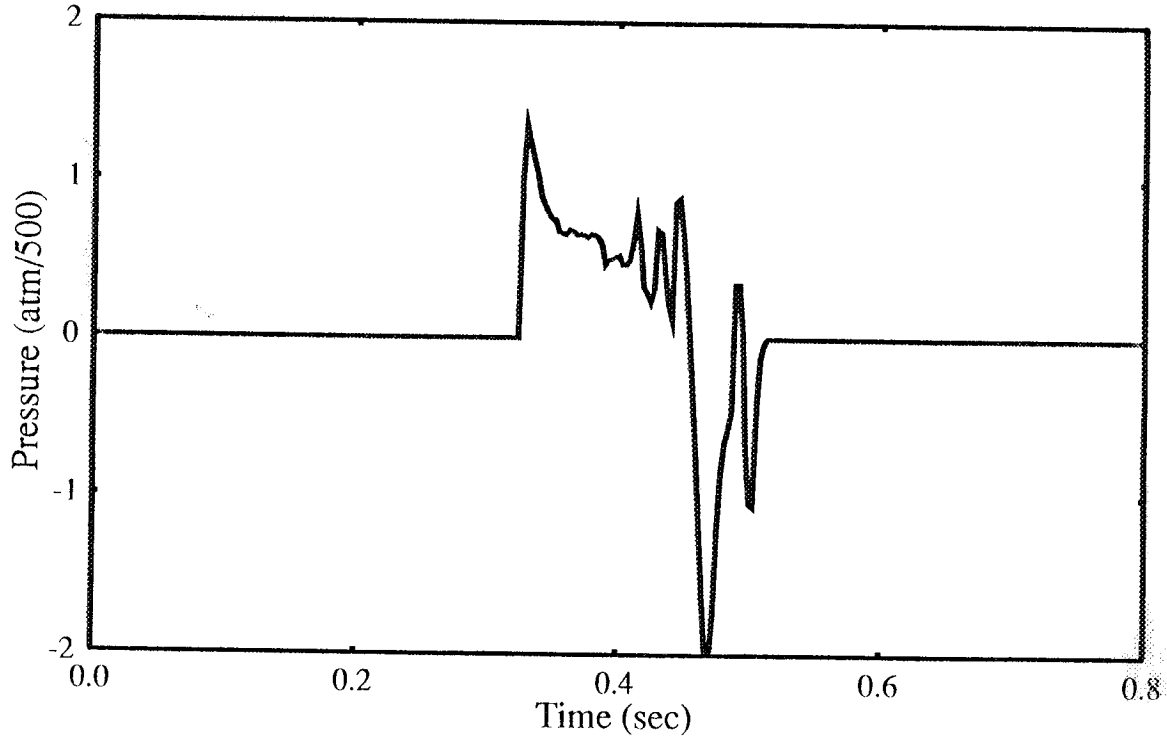

Figure 1. a.) Predicted HSCT waveform close to the aircraft.

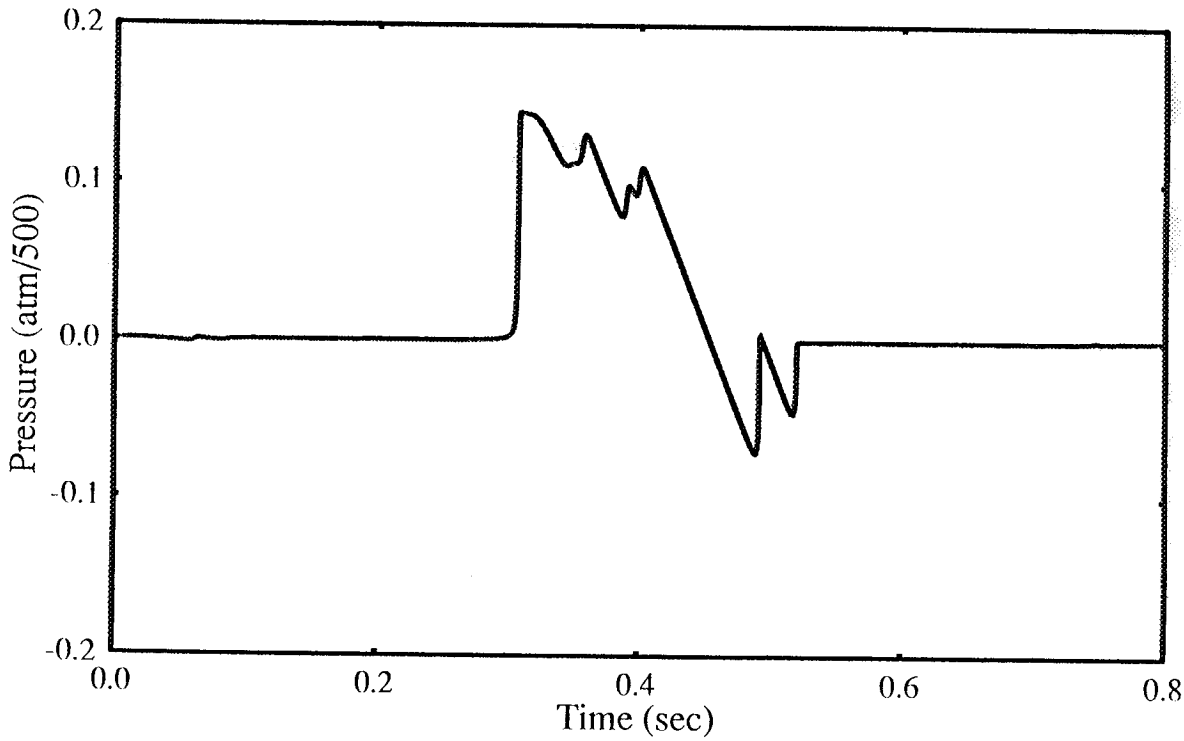

b.) HSCT waveform at the ground predicted using the enhanced Anderson algorithm.

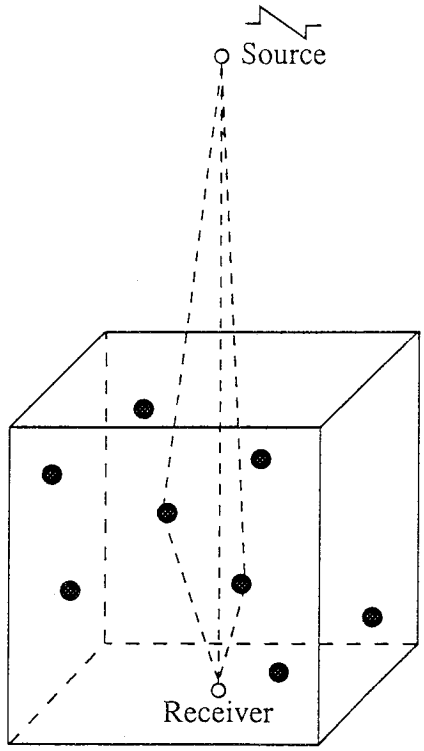

Figure 2. Scattering center calculation for sonic booms.

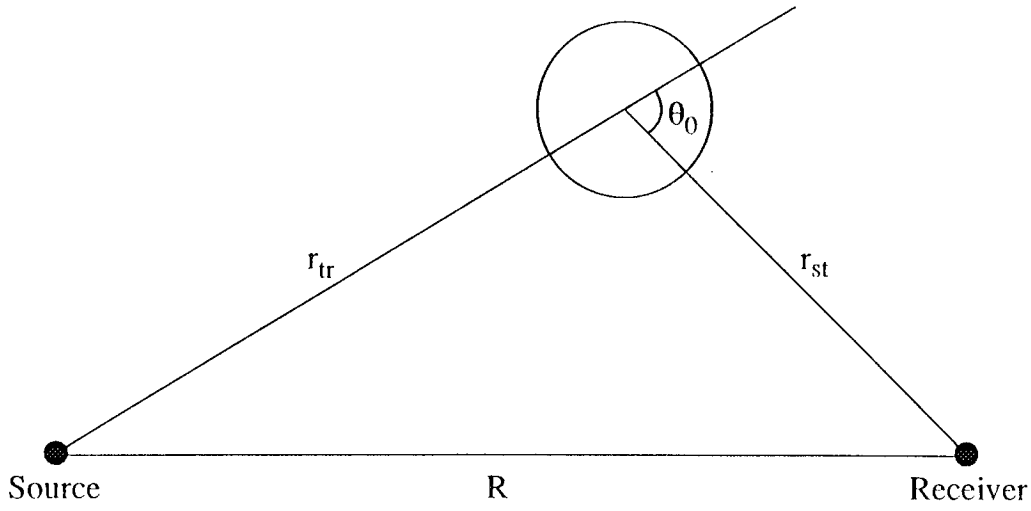

Figure 3. Geometry for the scattering calculation.

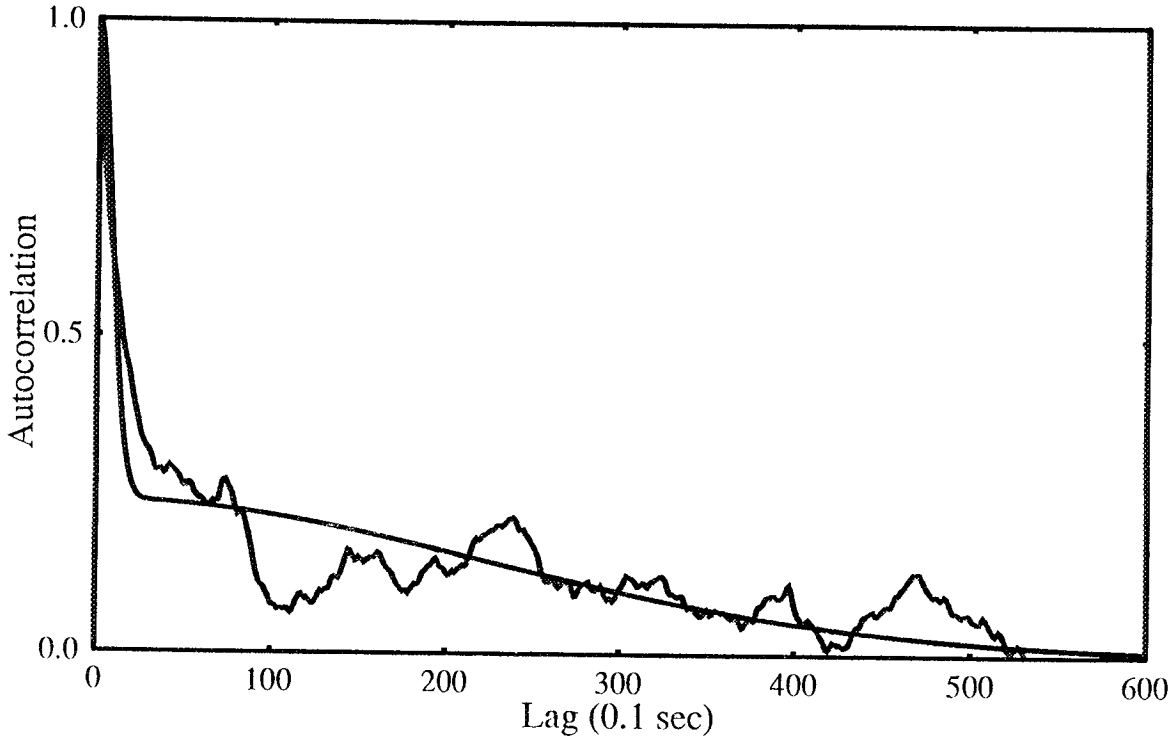

Figure 4. Two scale fit to the autocorrelation of the wind speed signal.

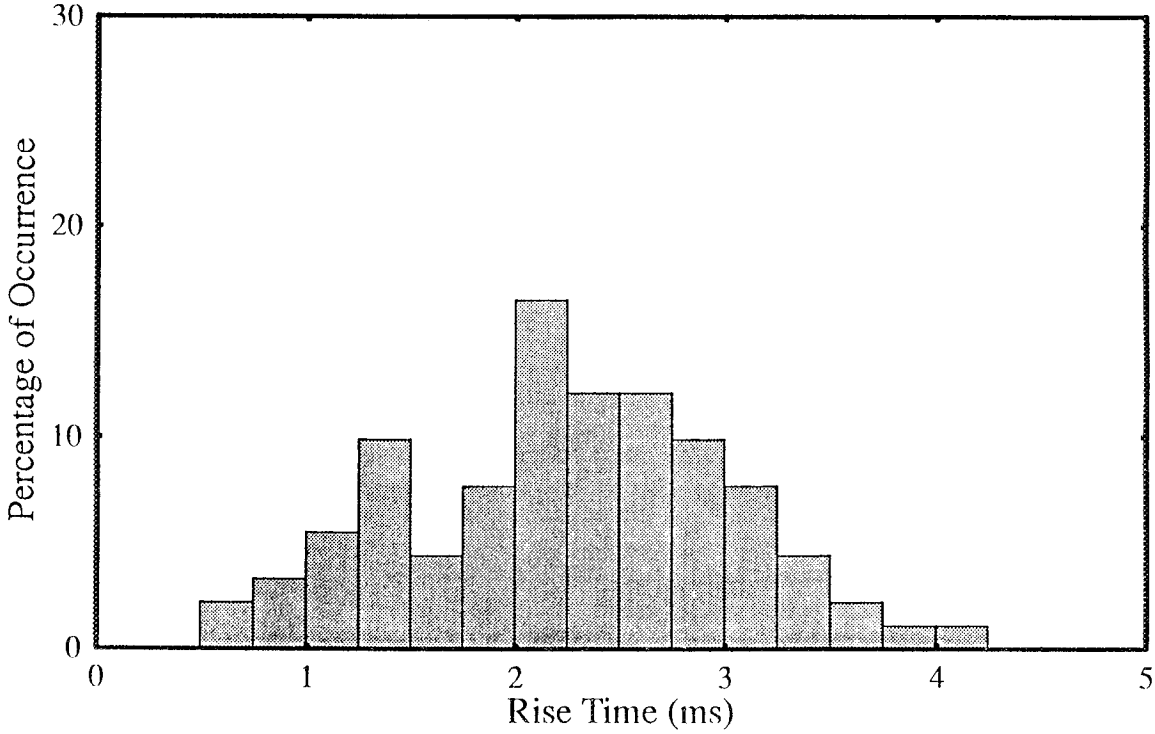

Figure 5. a.) Measured risetime distribution for the T-38 aircraft.

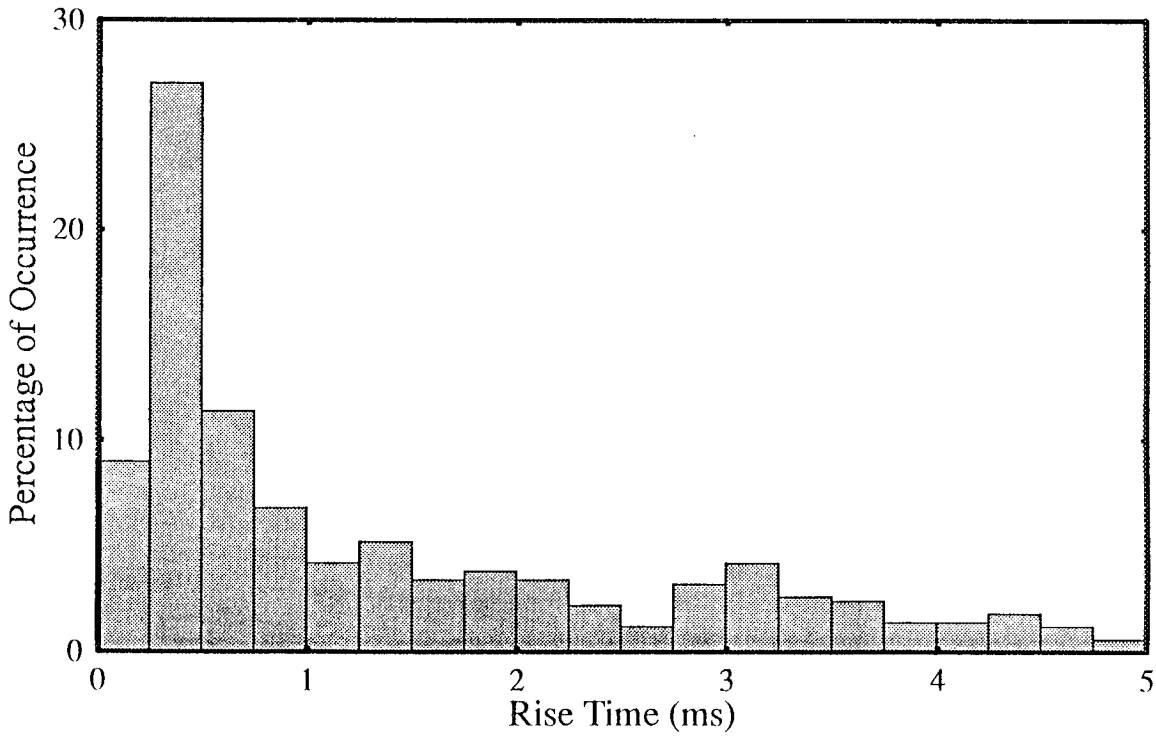

b.) Predicted distribution using the two scale model.

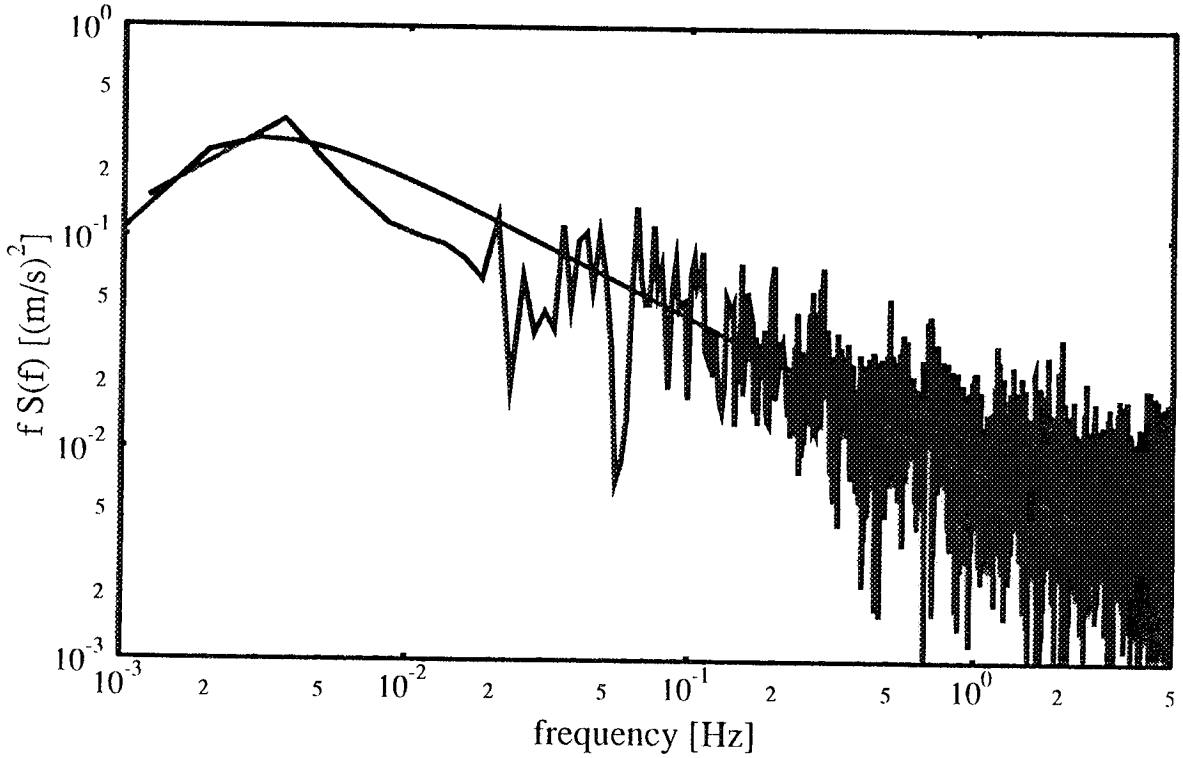

Figure 6. Fit of the von Karman spectrum to a 23 minute sample of wind data.

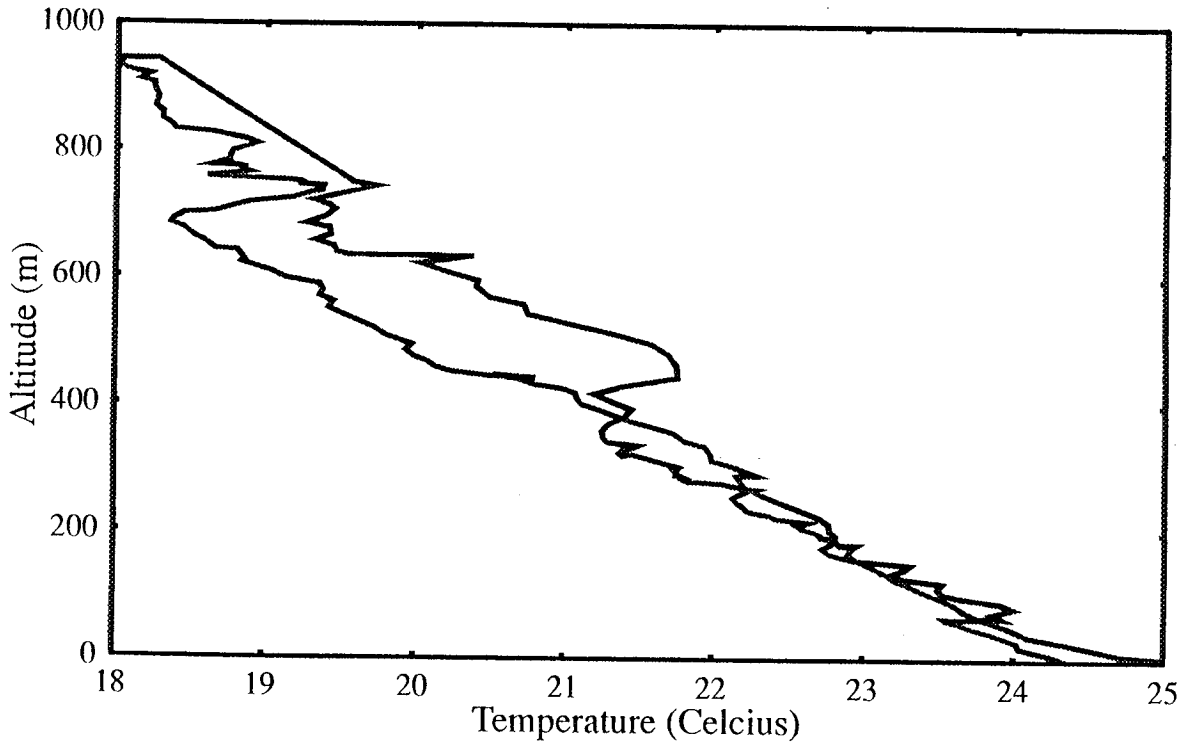

Figure 7. Temperature versus height for one flight at JAPE-2.

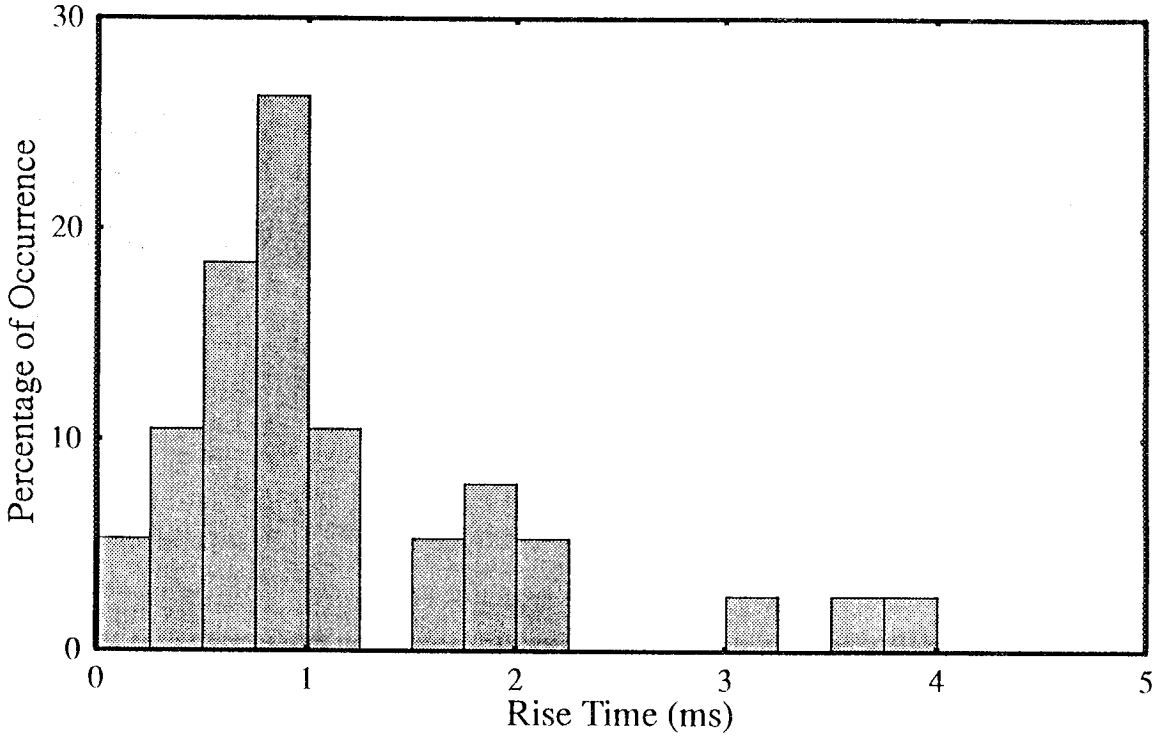

Figure 8. Prediction of risetime distribution using the von Karman spectrum. (20 realizations).